



Model-based analysis of water management in alkaline direct methanol fuel cells

C. Weinzierl ^{a, b}, U. Krewer ^{b,*}

^a Max Planck Institute for Dynamics of Complex Technical Systems, Sandtorstr. 1, 39106 Magdeburg, Germany¹

^b TU Braunschweig, Institute of Energy and Process Systems Engineering, Franz-Liszt-Str. 35, 38106 Braunschweig, Germany²



HIGHLIGHTS

- First modelling study of water management in anion exchange membrane ADMFCs.
- Water transport through membrane essential for operating anion exchange membrane FC.
- Required water diffusivity for sufficient water supply to cathode is identified.
- Considering the results will help to optimize new membrane material for AFC.

ARTICLE INFO

Article history:

Received 23 January 2014

Received in revised form

27 May 2014

Accepted 12 June 2014

Available online 7 July 2014

Keywords:

Methanol

Alkaline fuel cell

Water transport

Water management

Mathematical modelling

Anion exchange membrane

ABSTRACT

Mathematical modelling is used to analyse water management in Alkaline Direct Methanol Fuel Cells (ADMFCs) with an anion exchange membrane as electrolyte. Cathodic water supply is identified as one of the main challenges and investigated at different operation conditions. Two extreme case scenarios are modelled to study the feasible conditions for sufficient water supply. Scenario 1 reveals that water supply by cathodic inlet is insufficient and, thus, water transport through membrane is essential for ADMFC operation. The second scenario is used to analyse requirements on water transport through the membrane for different operation conditions. These requirements are influenced by current density, evaporation rate, methanol cross-over and electro-osmotic drag of water. Simulations indicate that water supply is mainly challenging for high current densities and demands on high water diffusion are intensified by water drag. Thus, current density might be limited by water transport through membrane. The presented results help to identify important effects and processes in ADMFCs with a polymer electrolyte membrane and to understand these processes. Furthermore, the requirements identified by modelling show the importance of considering water transport through membrane besides conductivity and methanol cross-over especially for designing new membrane materials.

© 2014 Elsevier B.V. All rights reserved.

1. Introduction

Recently, alkaline fuel cells (AFCs) attract attention by reason of their ability to operate with non-precious metals as catalyst. Due to higher stability and activity of non-precious metals in alkaline media compared to acidic media, it is possible to use metal catalyst in AFCs other than platinum (Pt), which is commonly used as

catalyst in low temperature fuel cells. Replacing Pt catalyst by other metal catalyst can reduce cost of fuel cells and, thus, is the main motivation to improve AFCs. Hence, research regarding AFC mostly focusses on new catalyst materials for oxygen reduction and oxidation of various fuels such as hydrogen, methanol, or other alcohols in alkaline media. A review about new catalyst for AFC can be found in Refs. [1,2].

Alkaline fuel cells are commonly operated using a liquid electrolyte such as potassium hydroxide (KOH) or sodium hydroxide (NaOH) which reacts with dissolved carbon dioxide (CO₂) according to Eq. (2) forming carbonate ions (CO₃²⁻):



* Corresponding author.

E-mail addresses: c.weinzierl@tu-braunschweig.de (C. Weinzierl), u.krewer@tu-braunschweig.de (U. Krewer).

¹ Address during research work.

² Present address.



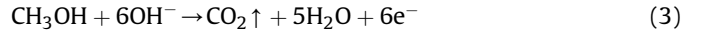
On one hand, this carbonation process decreases the performance of the fuel cell due to slower kinetics of fuel oxidation at anode [3] and lower ionic conductivity of the electrolyte [4]. On the other hand carbonates in supersaturated solutions can form precipitating salts (Eq. (2)) that may block pores of gas diffusion layer, catalyst layer or membrane. In order to avoid the disadvantages caused by carbonation of liquid electrolyte, anion exchange membranes were invented as a solid alkaline electrolyte [5]. It has been reported that similar performance of a fuel cell can be obtained with an alkaline anion exchange membrane (AAEM) in CO_3^- form and with the same AAEM in OH^- form [6]. Still, there are only few studies about AFCs using solely a solid electrolyte membrane instead of liquid electrolyte and most of them analyse cell performance for new membranes, ionomers or catalysts [7–11].

It has already been noticed that water transport through membrane might be a limiting factor [11]. Nevertheless, only little attention is given to process engineering issues like water transport through the membrane or water management so far. Diffusion coefficient and electro-osmotic drag coefficient of water through an anion exchange membrane were determined from experimental results by Ref. [12]. Likewise, the water diffusion coefficient through an anion exchange Morgan ADP membrane was estimated from sorption kinetics by Ref. [13]. A model based prediction of the water diffusion coefficient through a SnowPure Excellion I-200 anion exchange membrane is given in Ref. [14] and electro-osmotic water drag coefficients in alkaline media were also determined [15]. Water management has been analysed for AFCs with liquid electrolyte by Refs. [16,17]. These two studies are based on mathematical modelling and belong to the few modelling studies that consider water transport or management in AFCs [16–21]. Although water management in AFCs is even more challenging without liquid electrolyte due to the lack of the buffer function of alkaline solutions, water management has only been studied for the anode of anion exchange membrane fuel cells so far [20,21]. These two studies are using stationary [20] and dynamical [21] 3D modelling to analyse flooding of anode including the influence of changes in various operation conditions. Some modelling works about AFC contain analysis of fuel cell performance [22–26]. The latter is the only modelling study regarding alkaline direct methanol fuel cells (ADMFCs). Furthermore, another two model based studies regarding AFCs without liquid electrolyte were found in literature, both of them analysing the conductivity and water uptake of the AAEM [27,28]. Hence, there is a lack of knowledge and publications in literature regarding modelling and simulation of anion exchange membrane fuel cells, particularly related to water management at cathode and in the whole fuel cell. It is still unclear in which way and intensity water management influences and limits fuel cell performance and what can be done to improve water management and to widen the operation range of the fuel cell. The present study fills that gap by investigating limitation of current density by water management. Requirements on operation conditions and water transport are analysed in order to estimate conditions for stable operation. To our knowledge, this paper presents the first model based analysis of the water management in an ADMFC.

2. Functional principle of an ADMFC

As all fuel cells, ADMFCs convert chemical energy stored in a fuel directly into electric energy using electrochemical reactions. In the case of an ADMFC, methanol is used as fuel which reacts with

hydroxide ions (OH^-) in the electrochemical oxidation reaction at the anode producing water and carbon dioxide and releasing electrons:



At the cathode, OH^- -ions are produced in the electrochemical reduction reaction of oxygen:



Hence, the overall reaction is the same as in acidic direct methanol fuel cells:



During operation, electrons are transported from anode to cathode via an electric circuit whereas OH^- -ions are conducted by an electrolyte from cathode to anode.

Since CO_2 is permanently produced at the anode, the carbonation process is more intense in ADMFCs than in alkaline hydrogen fuel cells. Hence, it is important to replace the liquid electrolyte by a solid electrolyte membrane in ADMFCs. A schematic of an ADMFC with a solid electrolyte membrane is shown in Fig. 1. The anode is fed with a methanol water solution while the cathode is flushed with air. Although the reactants are separated by a membrane, some mass transport through the membrane takes place in addition to the ionic transport. Methanol transported through the membrane by diffusion, hereafter named as methanol cross-over, is oxidised at the cathode in a chemical reaction similar to the overall reaction Eq. (5) producing water. This loss of methanol decreases the efficiency of the fuel cell. Furthermore, the methanol oxidation at the cathode causes a decrease in cell potential due to a mixed potential [29]. Similar to methanol, water is also diffusing through the membrane from anode to cathode but

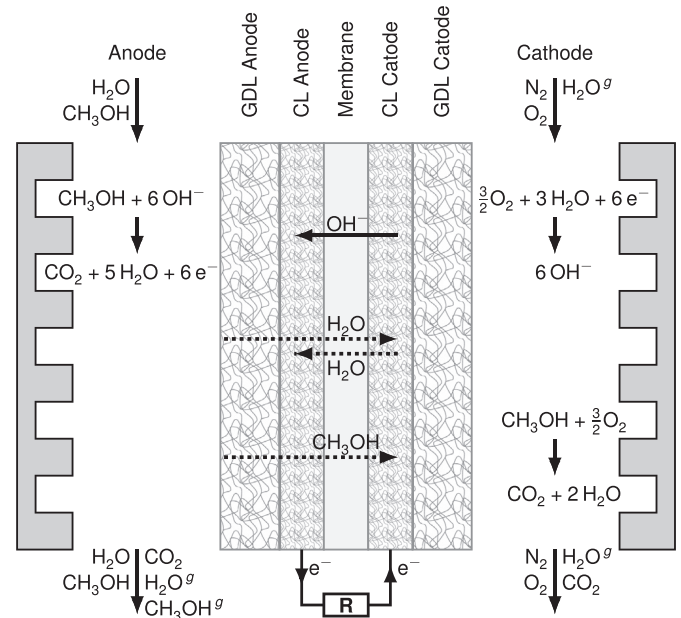


Fig. 1. Schematic of an ADMFC including anode and cathode fluid channels, gas diffusion layers (GDLs), catalyst layers (CLs) and a solid electrolyte membrane.

there is also a back transport by electro-osmotic water drag caused by the ionic transport. Hence, water is consumed at the gas flushed cathode due to the reduction reaction Eq. (4) and electro-osmotic water drag. Thus, water has to be supplied to the cathode to provide sufficient amount of water for the electrochemical reaction. At the same time, water is added to the liquid flow at the anode due to the electrochemical oxidation reaction Eq. (3) and the water drag.

All these information lead to the conclusion that water management in ADMFCs is challenging at both electrodes of the fuel cell. This paper focuses on water management to enable stable cathode performance by analysing one big challenge regarding water management in ADMFCs: the cathodic water supply.

3. General mathematical model

In this study, mathematical modelling is used to describe and analyse processes and water management in an ADMFC. For that reason, the following general model is derived which is modified later forming different scenarios. The two scenarios analysed in this paper solely describe a single fuel cell which is sketched in Fig. 2. The membrane which couples anode and cathode is not modelled in detail, but it is implemented as a semipermeable wall that allows transport of certain species. In order to focus on the important processes, the model is kept as simple as possible by including the following assumptions.

Pressure and temperature at anode and cathode are assumed to be constant at 1 bar and 323.15 K, respectively. Therefore, it is not necessary to include an energy balance. Furthermore, charge balances are not considered since the model is not used to study the performance but to analyse procedural requirements. Hence, the

differential equations of this model arise from mass balances of the components β with the space direction k .

$$\frac{\partial \rho_\beta}{\partial t} = -\frac{\partial}{\partial z_k} (\rho_\beta v_k + j_{k,\beta}) + \sigma_\beta^* \quad (6)$$

The model is used to analyse overall water management of the whole fuel cell in order to investigate conditions that are at least required for sufficient water supply to the cathode. The minimum requirements can be obtained by assuming an ideal system in which transport processes within the chambers e.g. through gas diffusion layer (GDL) and catalyst layer (CL) are disregarded. Thus, it is assumed that no local gradients appear in anode and cathode chamber which are modelled as continuous stirred tank reactors (CSTRs). The consequences of this assumption are discussed for each scenario separately. Furthermore, diffusion through membrane is described by Fick's law. Methanol (Me) diffusing through the membrane is immediately oxidised at the cathodic catalyst layer as well as liquid water is immediately consumed or evaporated at the cathode ($c_{\beta,\text{liq}}^C = 0$). Water drag takes place from cathode to anode ($\dot{n}_{\text{H}_2\text{O}}^{\text{drag}}$) while it is assumed that no methanol is dragged by ions. Thus, the mass balances for all components $\beta \in \{\text{Me}, \text{H}_2\text{O}, \text{Me}^g, \text{H}_2\text{O}^g, \text{CO}_2, \text{O}_2, \text{N}_2\}$ reduce to:

$$V^A \frac{dc_\beta^A}{dt} = \dot{n}_{\beta,\text{in}}^A - \dot{n}_{\beta,\text{out}}^A - \dot{n}_{\beta,\text{drag}}^A + \sigma_\beta^A \quad (7)$$

$$V^C \frac{dc_\beta^C}{dt} = \dot{n}_{\beta,\text{in}}^C - \dot{n}_{\beta,\text{out}}^C + \dot{n}_{\beta,\text{drag}}^C + \sigma_\beta^C \quad (8)$$

$$\text{with } \dot{n}_{\beta,\text{out}}^l = c_\beta^l F_{\text{out}}^l \quad (9)$$

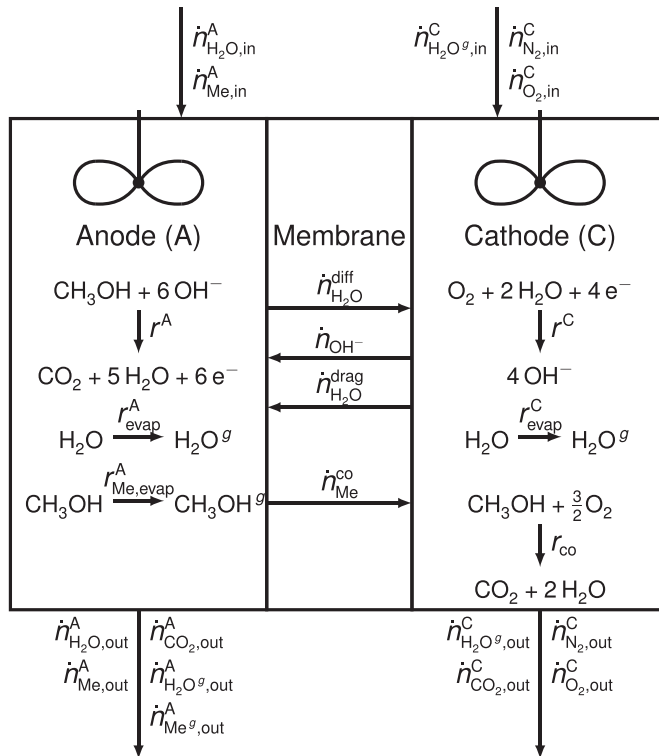


Fig. 2. Sketch of the general model of an ADMFC. The chambers are well mixed (no local gradients) and the membrane allows transport of certain species.

Neglecting mixing volumes, the volume flows leaving anode and cathode can be derived from the overall mass balances in the chambers:

$$F_{\text{out}}^A = F_{\text{in}}^A - \frac{\dot{n}_{\text{H}_2\text{O}}^{\text{diff}}}{c_{\text{H}_2\text{O}}^*} - \frac{\dot{n}_{\text{Me}}^{\text{co}}}{c_{\text{Me}}^*} + \sum_\alpha \frac{\sigma_\alpha^A}{c_\alpha^*} \quad (11)$$

$$F_{\text{out}}^C = \frac{p_{\text{in}}^C T_{\text{in}}^C}{p_{\text{out}}^C T_{\text{out}}^C} F_{\text{in}}^C + \frac{\dot{n}_{\text{H}_2\text{O}}^{\text{diff}}}{c_{\text{H}_2\text{O}^g}^*} + \sum_\gamma \frac{\sigma_\gamma^C}{c_\gamma^*} \quad (12)$$

with $\dot{n}_{\text{Me}}^{\text{co}} = \dot{n}_{\text{Me}}^{\text{diff}}$ and $c_{\alpha/\gamma}^*$ being the concentration of the pure substance of component α at anode or γ at cathode and $\alpha \in \{\text{Me}, \text{H}_2\text{O}, \text{Me}^g, \text{H}_2\text{O}^g, \text{CO}_2\}$ as well as $\gamma \in \{\text{H}_2\text{O}^g, \text{CO}_2, \text{O}_2, \text{N}_2\}$. The inlet flow rates at anode and cathode are defined by consumption of the reactant proportional to an excess ratio λ which is kept constant in order to avoid reactant starvation. Consequently, volume flow rates change with current density (Eqs. (A.20) and (A.21)).

Since the model is not used to analyse dynamics or system performance, the kinetics of reactions are disregarded and reaction rates are described by Faraday's law. It is further assumed that gas and liquid at anode are always in equilibrium. For the calculation of the molar fractions of water in the gas phase $y_{\text{H}_2\text{O}^g}$, the laws of Raoult and Dalton are used as well as the ideal gas law and the

Wagner equation [30]. The corresponding equations are declared in A. Thus, the resulting sources and sinks σ_β at anode and cathode in Eqs. (7) and (8), which are caused by reaction, evaporation and electro-osmotic drag, can be expressed by:

$$\sigma_{\text{Me}}^A = -\frac{A^M i}{6F} - \frac{y_{\text{Me}^g}^A}{1 - y_{\text{Me}^g}^A - y_{\text{H}_2\text{O}^g}^A} \frac{A^M i}{6F} \quad (13)$$

$$\sigma_{\text{H}_2\text{O}}^A = \frac{5A^M i}{6F} - \frac{y_{\text{H}_2\text{O}^g}^A}{1 - y_{\text{Me}^g}^A - y_{\text{H}_2\text{O}^g}^A} \frac{A^M i}{6F} + \kappa \frac{A^M i}{F} \quad (14)$$

$$\sigma_{\text{CO}_2}^A = \frac{A^M i}{6F} \quad (15)$$

$$\sigma_{\text{Me}^g}^A = \frac{y_{\text{Me}^g}^A}{1 - y_{\text{Me}^g}^A - y_{\text{H}_2\text{O}^g}^A} \frac{A^M i}{6F} \quad (16)$$

$$\sigma_{\text{H}_2\text{O}^g}^A = \frac{y_{\text{H}_2\text{O}^g}^A}{1 - y_{\text{Me}^g}^A - y_{\text{H}_2\text{O}^g}^A} \frac{A^M i}{6F} \quad (17)$$

$$\sigma_{\text{N}_2}^C = 0 \quad (18)$$

$$\sigma_{\text{O}_2}^C = -\frac{A^M i}{4F} - \frac{3}{2} \dot{n}_{\text{Me}}^{\text{co}} \quad (19)$$

$$\sigma_{\text{H}_2\text{O}^g}^C = -\frac{A^M i}{2F} + 2\dot{n}_{\text{Me}}^{\text{co}} - \kappa \frac{A^M i}{F} \quad (20)$$

$$\sigma_{\text{CO}_2}^C = \dot{n}_{\text{Me}}^{\text{co}} \quad (21)$$

Further equations that complement the model are listed in Appendix A.

The parameters and initial conditions listed in Tables 1–3 are used for the simulation of both scenarios unless specified differently.

4. Modelling and analysis of different scenarios for cathodic water supply

The general mathematical model above is modified to describe different scenarios for the analysis of the water management in

Table 1
Chemical data used for simulation of all scenarios.

Parameter	Value	Parameter	Value
A_{Me}	−8.54582	M_{Me}	32.04 g mol ^{−1}
B_{Me}	0.67266	$M_{\text{H}_2\text{O}}$	18.02 g mol ^{−1}
C_{Me}	−2.54743	M_{CO_2}	44.01 g mol ^{−1}
D_{Me}	−2.71874	M_{O_2}	32.00 g mol ^{−1}
$A_{\text{H}_2\text{O}}$	−7.71374	c_{Me}^*	24.66 mol l ^{−1}
$B_{\text{H}_2\text{O}}$	1.31467	$c_{\text{H}_2\text{O}}^*$	55.4 mol l ^{−1}
$C_{\text{H}_2\text{O}}$	−2.51444	κ	4
$D_{\text{H}_2\text{O}}$	−1.72542	D_{Me}^M	$1.23 \cdot 10^{-7} \text{ cm}^2 \text{ s}^{-1}$
$T_{\text{Me}}^{\text{crit}}$	512.5 K	$p_{\text{Me}}^{\text{crit}}$	$80.8 \cdot 10^5 \text{ Pa}$
$T_{\text{H}_2\text{O}}^{\text{crit}}$	647.1 K	$p_{\text{H}_2\text{O}}^{\text{crit}}$	$220.6 \cdot 10^5 \text{ Pa}$

Table 2
Physical constants and geometry parameters used for simulation of all scenarios.

Parameter	Value	Parameter	Value
F	96,485 A s mol ^{−1}	R	$8.31 \text{ J mol}^{-1} \text{ K}^{-1}$
V^A	12.5 ml	V^C	12.5 ml
A^M	25 cm ²	d^M	30 μm

ADMFCs. In this paper, conditions for sufficient water supply to the cathode are studied. Therefore, the following two scenarios are created that fulfil cathodic water demand in various ways. In order to keep the models as simple as possible, these scenarios only describe a single fuel cell fed with a methanol solution of 1 mol l^{−1} and a constant excess ratio λ^A . Hence, the molar flows entering the anode are time-independent, $\dot{n}_{\alpha,\text{in}}^A \neq f(t)$ but do change with current density. Both scenarios are simulated using Matlab. In the first scenario, the algebraic equations displayed below are calculated straightforward. In order to be more flexible in extending and modifying the model, the second scenario is numerically integrated for various current densities with the solver ode15s of Matlab until steady state is reached. The steady state results are shown in this study. These results are same if solver ode45 of Matlab is used for the numerical integration. However, it would also be possible to calculate the steady state concentrations by solving a complex system of algebraic equations which leads to the same results as the numerical integration.

In the first scenario, water is supplied by humidifying cathodic inlet gas. This scenario is used to analyse which inlet conditions lead to sufficient water supply. In the second scenario, water is supplied by mass transport through membrane to analyse the requirements on water diffusion for sufficient water supply.

4.1. Scenario 1 – water supply by cathodic inlet

This scenario is used to identify inlet conditions that lead to sufficient water supply. Therefore, a mathematical model is presented first, followed by the discussion of the results.

4.1.1. Mathematical modelling

In order to study the effect of water supply by solely humidifying the cathodic inlet gas, molar flows through the membrane are assumed to be zero ($\dot{n}_{\text{H}_2\text{O}}^{\text{diff}} = \dot{n}_{\text{H}_2\text{O}}^{\text{drag}} = \dot{n}_{\text{Me}}^{\text{co}} = 0$). This is implemented by setting the corresponding coefficients equal to zero: $\kappa = 0$, $D_\beta^M = 0$ for $\beta \in \{\text{Me}, \text{H}_2\text{O}\}$. Hence, anode and cathode are decoupled and it is sufficient to consider only the cathode for the analysis of this

Table 3
Operation conditions used for simulation of all scenarios.

Anode:		Cathode	
Parameter	Value	Parameter	Value
p^A	1.013 bar	p^C	1.013 bar
T^A	323.15 K	T^C	323.15 K
RH^A	100%		
$c_{\text{Me},0}^A$	1 mol l ^{−1}	$c_{\text{O}_2,0}^C$	$7.92 \cdot 10^{-3} \text{ mol l}^{-1}$
$c_{\text{H}_2\text{O},0}^A$	53.15 mol l ^{−1}	$c_{\text{N}_2,0}^C$	$29.8 \cdot 10^{-3} \text{ mol l}^{-1}$
$c_{\text{O}_2,0}^A$	0 mol l ^{−1}	$c_{\text{CO}_2,0}^C$	0 mol l ^{−1}
$c_{\text{Me}^*,0}^A$	0 mol l ^{−1}	$c_{\text{H}_2\text{O}^*,0}^C$	0 mol l ^{−1}
$c_{\text{H}_2\text{O}^*,0}^A$	0 mol l ^{−1}	T_{in}^C	293 K
$c_{\text{Me,in}}^A$	1 mol l ^{−1}	p_{in}^C	1.013 bar
$c_{\text{H}_2\text{O,in}}^A$	53.15 mol l ^{−1}	λ^C	10
$c_{\text{O}_2,in}^A$	0 mol l ^{−1}	$c_{\text{CO}_2,in}^C$	0 mol l ^{−1}
$c_{\text{Me}^*,in}^A$	0 mol l ^{−1}		
$c_{\text{H}_2\text{O}^*,in}^A$	0 mol l ^{−1}		

scenario. Furthermore, it is assumed that the gas entering the cathode is saturated with water. Considering these assumptions, the mass balance, Eq. (8), for cathodic water in steady state can be reduced to:

$$0 = \dot{n}_{\text{H}_2\text{O}^g,\text{in}}^{\text{C}} - c_{\text{H}_2\text{O}^g}^{\text{C}} F_{\text{out}}^{\text{C}} + \sigma_{\text{H}_2\text{O}^g}^{\text{C}} \quad (22)$$

With $\kappa = 0$ and $D_{\beta}^{\text{M}} = 0$, Eqs. (19)–(21) can be modified as follows:

$$\sigma_{\text{O}_2}^{\text{C}} = -\frac{A^{\text{M}} i}{4F} \quad (23)$$

$$\sigma_{\text{H}_2\text{O}^g}^{\text{C}} = -\frac{A^{\text{M}} i}{2F} \quad (24)$$

$$\sigma_{\text{CO}_2}^{\text{C}} = 0 \quad (25)$$

Including Eq. (12) for $\dot{n}_{\text{H}_2\text{O}^g}^{\text{diff}} = 0$, Eqs. (23)–(25), (A.21), (A.11) and (A.12) into Eq. (22) results in an equation to calculate the air excess ratio λ^{C} required to supply sufficient water. A detailed derivation of this equation can be found in the appendix (A.25):

$$\lambda^{\text{C}} = \frac{2 - 3 \frac{c_{\text{H}_2\text{O}^g}^{\text{C}}}{c_{\text{gas}}^{\text{C}}}}{y_{\text{H}_2\text{O}^g,\text{in}}^{\text{C}} - \frac{c_{\text{H}_2\text{O}^g}^{\text{C}}}{c_{\text{gas}}^{\text{C}}}} \left(0.21 \left(1 - y_{\text{H}_2\text{O}^g,\text{in}}^{\text{C}} \right) \right) \quad (26)$$

with the mole fraction of water at the cathodic inlet $y_{\text{H}_2\text{O},\text{in}}^{\text{C}}$ and the water concentration $c_{\text{H}_2\text{O}^g}^{\text{C}}$ at the cathodic outlet. For ideal gases, the corresponding norm volume flow rate at cathodic inlet can be calculated as:

$$F_{\text{in},\text{N}}^{\text{C}} = \frac{RT_{\text{N}} \dot{n}_{\text{in}}^{\text{C}}}{p_{\text{N}}} \quad (27)$$

Including Eqs. (A.17) and (A.19) results in:

$$F_{\text{in},\text{N}}^{\text{C}} = \frac{RT_{\text{N}}}{p_{\text{N}}} \frac{1}{0.21 \left(1 - y_{\text{H}_2\text{O},\text{in}}^{\text{C}} \right)} \frac{I}{4F} \lambda^{\text{C}} \quad (28)$$

Additional parameters needed to simulate the model of this scenario are listed in Table 4.

4.1.2. Results and discussion

Since this scenario is only considering the cathode of the fuel cell, the results shown below can be applied to all alkaline fuel cells fed with air at the cathode.

Fig. 3 shows the minimum air excess ratio required to supply sufficient water at the cathode as a function of inlet temperature for $RH_{\text{in}}^{\text{C}} = 100\%$. The limiting curve that assumes total water consumption ($c_{\text{H}_2\text{O}}^{\text{C}} = 0$) decreases with increasing inlet temperature. This curve is independent of current density. Below the curve, water supply is insufficient, above the curve some water remains in

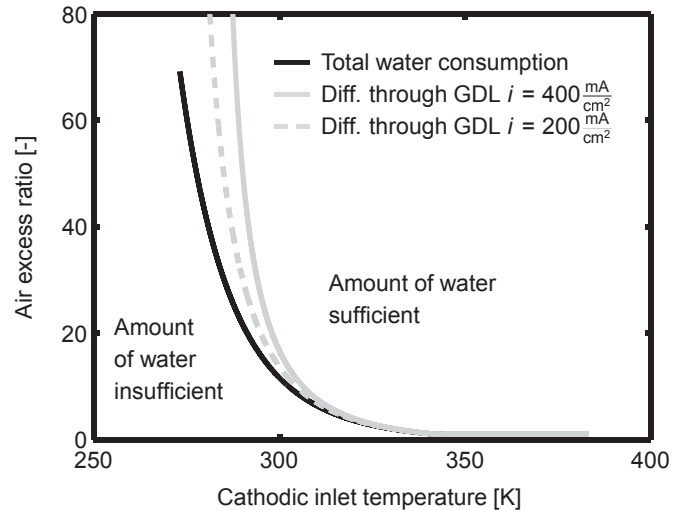


Fig. 3. Required air excess ratio for sufficient water supply by cathodic inlet gas as a function of inlet temperature for total water consumption and considering diffusion through a GDL of thickness $d_{\text{GDL}} = 300 \mu\text{m}$ at a current density of $i = 200 \text{ mA cm}^{-2}$ and $i = 400 \text{ mA cm}^{-2}$ respectively.

the cathodic gas. Further limitations due to mass transport and dehumidification kinetics which inhibit total dehumidification intensify the requirements. This is indicated by the grey curves in Fig. 3 which include water vapour transport through a GDL of $300 \mu\text{m}$ thickness at a current density of $i = 200 \text{ mA cm}^{-2}$ and $i = 400 \text{ mA cm}^{-2}$ respectively. The remaining water concentration in the cathode chamber $c_{\text{H}_2\text{O}}^{\text{C}}$ is then calculated by Eq. (A.22). The results show that high inlet temperatures are required to supply sufficient water for reasonable air excess ratios if mass transport through membrane does not occur. This is intensified by considering limitation due to mass transport from chamber through GDL to reaction region. This mass transport is proportional to current density. Thus, if the transport of water vapour through GDL is considered, higher current density necessitates higher water diffusion and, thus, requires higher water vapour concentration at cathode. Therefore, higher current densities lead to higher air excess ratios required for sufficient water supply.

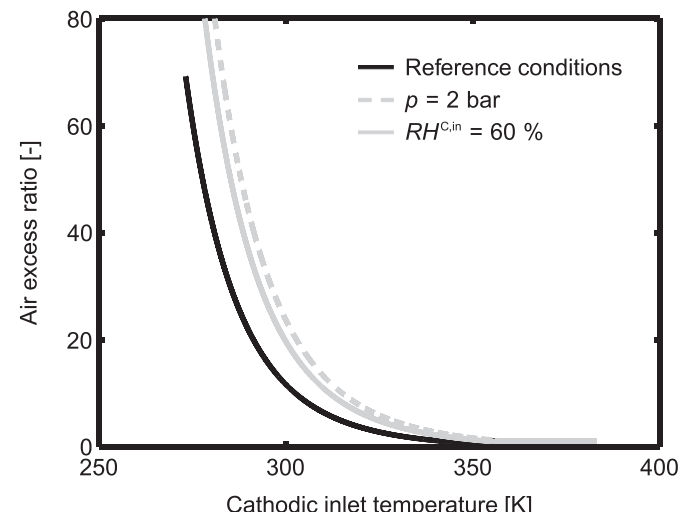


Fig. 4. Required air excess ratio for sufficient water supply by cathodic inlet gas as a function of inlet temperature for total water consumption at reference conditions: all gas pressures are $p = 1 \text{ bar}$ and $RH_{\text{in}}^{\text{C}} = 100\%$; and at $p = 2 \text{ bar}$ as well as for $RH_{\text{in}}^{\text{C}} = 60\%$.

Table 4
Additional parameters used for simulation of scenario 1.

Parameter	Value	Parameter	Value
d_{GDL}	300 μm	i	400 mA cm^{-2}
$D_{\text{H}_2\text{O}}^{\text{GDL}}$	0.15 $\text{cm}^2 \text{s}^{-1}$	$RH_{\text{in}}^{\text{C}}$	100%
T_{N}	273.15 K	p_{N}	1.013 bar

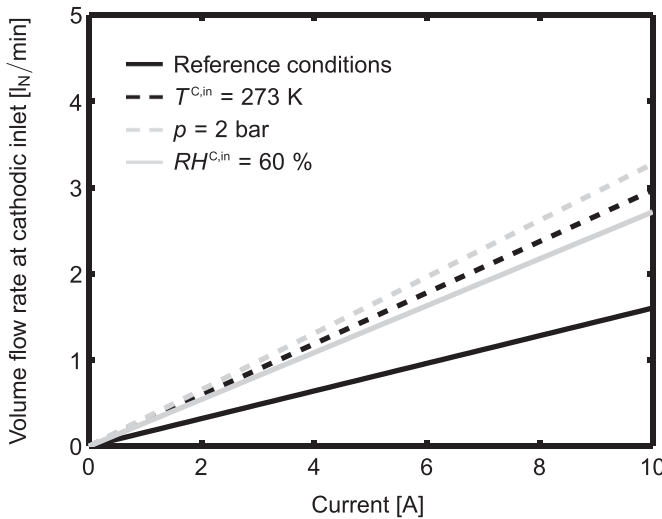


Fig. 5. Required inlet volume flow rate of air for sufficient water supply by cathodic inlet gas as a function of current for total water consumption at reference conditions: $T_{\text{in}}^{\text{C}} = 300 \text{ K}$, $\text{RH}_{\text{in}}^{\text{C}} = 100\%$ and $p = 1.013 \text{ bar}$, and at $T_{\text{in}}^{\text{C}} = 273 \text{ K}$, at $p = 2.026 \text{ bar}$ and at $\text{RH}_{\text{in}}^{\text{C}} = 60\%$.

Fig. 4 reveals the influence of pressure and relative humidity. All three curves in this figure assume total water consumption at cathode. The reference conditions include that pressure at cathode and cathodic inlet is $p^{\text{C}} = p_{\text{in}}^{\text{C}} = p = 1.013 \text{ bar}$ and the relative humidity at cathodic inlet is $\text{RH}_{\text{in}}^{\text{C}} = 100\%$. These conditions are in accordance with the conditions of the black curve in **Fig. 3**. A pressure increase, e.g. to $p = 2.026 \text{ bar}$, necessitates higher values of air excess ratio in order to supply sufficient water. The same impact is observed if the relative humidity of air at cathodic inlet is lowered, e.g. to $\text{RH}_{\text{in}}^{\text{C}} = 60\%$. That is because in both cases the amount of water in the inlet air is lower and, thus, more air needs to be fed to the fuel cell to provide sufficient water.

The required air excess ratios in **Fig. 4** are not influenced by current produced by the fuel cell. However, the corresponding volume flow rates which are calculated by Eq. (28) for the same conditions do increase with current as shown in **Fig. 5**. A norm volume flow rate of approximately $V_{\text{in},N}^{\text{C}} = 1.6 \text{ l}_N \text{ min}^{-1}$ is required to supply sufficient water to produce a current of $I = 10 \text{ A}$ at reference conditions. A decrease of inlet temperature to $T_{\text{in}}^{\text{C}} = 273 \text{ K}$ results in a volume flow rate of $V_{\text{in},N}^{\text{C}} = 3 \text{ l}_N \text{ min}^{-1}$. The volume flows required in the cases of higher pressure ($p = 2.026 \text{ bar}$) and lower humidity ($\text{RH}_{\text{in}}^{\text{C}} = 60\%$) are also approximately double of that at reference conditions. Hence, for low inlet temperatures, unreasonably high volume flow rates at cathodic inlet are required for high currents, while cathodic water supply seems feasible for low currents.

In conclusion, the air needs to be humidified and either high inlet temperatures or high volume flow rates at cathodic inlet are required in order to supply sufficient water to cathode. These two options require additional components, e.g. humidifier and heater, which significantly complicate the fuel cell system and which are detrimental to system efficiency. Hence, this scenario reveals that water supply by cathodic inlet is insufficient and mass transport through membrane is essential for cathodic water supply in alkaline fuel cells.

4.2. Scenario 2 – water supply by mass transport through membrane

This scenario is used to study the requirements on the water diffusion through membrane for sufficient cathodic water supply.

Therefore, the general model is slightly modified and afterwards the results are discussed.

4.2.1. Mathematical modelling

Water is supplied at cathode by oxidation of methanol diffusing through membrane as well as directly by water diffusion from anode to cathode. In order to analyse the requirements on water transport through membrane for sufficient water supply, the corresponding diffusion coefficient that exactly satisfies cathodic water demand can be derived from Eq. (8) for water in steady state:

$$D_{\text{H}_2\text{O}}^{\text{M}} = \left(c_{\text{H}_2\text{O}}^{\text{C}} F_{\text{out}}^{\text{C}} - \dot{n}_{\text{H}_2\text{O,in}}^{\text{C}} - \sigma_{\text{H}_2\text{O}}^{\text{C}} \right) \frac{d^{\text{M}}}{A^{\text{M}} c_{\text{H}_2\text{O}}^{\text{A}}} \quad (29)$$

Instead of humidifying cathodic inlet gas, ambient air is used at $T_{\text{in}}^{\text{C}} = 293 \text{ K}$ and $\text{RH}_{\text{in}}^{\text{C}} = 60\%$. As such, gas in the cathode chamber does not supply water for the electrochemical reaction. On the contrary, it is assumed that either some of the available water is evaporated and, thus, lost for reaction or the water content of the gas does not change at all. In order to analyse the effect of electro-osmotic water drag, methanol cross-over and evaporation at cathode, these processes are switched off one by one and the results are compared to the reference conditions in which all processes occur. Hence, scenario 2 is analysed for the following conditions: With electro-osmotic water drag $\kappa = 4$ or without $\kappa = 0$, with methanol cross-over $D_{\text{Me}}^{\text{M}} = 1.23 \cdot 10^{-7} \text{ cm}^2 \text{ s}^{-1}$ or without $D_{\text{Me}}^{\text{M}} = 0$, with evaporation at cathode to $\text{RH}_{\text{in}}^{\text{C}} = 100\%$ at $T^{\text{C}} = 323 \text{ K}$, $\dot{n}_{\text{H}_2\text{O,out}}^{\text{C}} > \dot{n}_{\text{H}_2\text{O,in}}^{\text{C}}$ or without evaporation $\dot{n}_{\text{H}_2\text{O,out}}^{\text{C}} = \dot{n}_{\text{H}_2\text{O,in}}^{\text{C}}$ and for different air excess ratios λ^{C} .

Several sources and sinks of water change the amount of water at anode. In the following, water accumulation $\Delta \dot{V}_{\text{H}_2\text{O}}$ denotes the difference between the volume of liquid water leaving the anode and the volume of liquid water fed to the anode.

$$\Delta \dot{V}_{\text{H}_2\text{O}} = F_{\text{H}_2\text{O,out}}^{\text{A}} - F_{\text{H}_2\text{O,in}}^{\text{A}} = \frac{\dot{n}_{\text{H}_2\text{O,out}}^{\text{A}} - \dot{n}_{\text{H}_2\text{O,in}}^{\text{A}}}{c_{\text{H}_2\text{O}}^{\text{A}}} \quad (30)$$

Additional parameters needed to simulate the model of this scenario are listed in **Table 5**.

4.2.2. Results and discussion

Fig. 6 displays the required diffusion coefficient of water calculated by Eq. (29) for reference conditions in which water drag, methanol cross-over and evaporation occur and $\lambda^{\text{C}} = 10$. It further shows four other cases which differ from the reference condition in one of the above mentioned conditions each.

In all cases, the required water diffusion coefficient increases with current density since a higher current leads to increased water consumption. Thus, regarding water transport through membrane, the cathodic water supply is mainly a challenge for high current densities. A significant influence of electro-osmotic water drag and evaporation can be observed while the diffusion coefficient is insignificantly higher without methanol cross-over for a methanol concentration of 1 mol l^{-1} at anodic inlet. The case without evaporation is per se independent of air excess ratio. In the case that

Table 5

Additional parameters used for simulation of scenario 2.

Parameter	Value	Parameter	Value
λ^{A}	4	$\text{RH}_{\text{in}}^{\text{C}}$	60%
λ^{C}	10	$\text{RH}_{\text{in}}^{\text{C}}$	100%

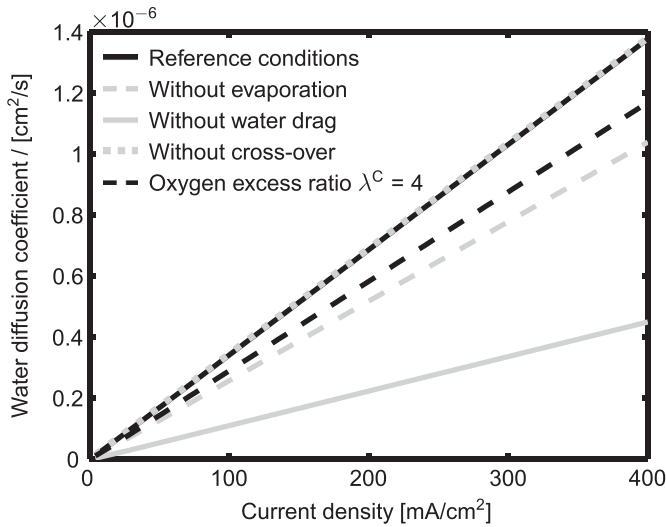


Fig. 6. Required water diffusion coefficient in scenario 2 at reference conditions: Including electro-osmotic water drag, methanol cross-over and evaporation at cathode with an air excess ratio of $\lambda^C = 10$; and for four other cases that differ from reference conditions in one of the mentioned conditions.

evaporation occurs, the required water diffusion coefficient decreases with decreasing air excess ratio. Thus, the influence of evaporation is reduced in case of a smaller air excess ratio.

Mass transport through GDL and CL which is disregarded in this study would of course influence these results. At cathode, a diffusive transport of water from CL to cathode chamber would lead to lower evaporation rates and, thus, to lower required diffusion coefficient. Hence, the required diffusion coefficient in real fuel cells lies in between the cases of no evaporation and full evaporation. At anode, water is in excess and is produced by reaction in the CL but concentration of methanol would decrease and cross-over would decrease accordingly. However, the influence of methanol cross-over on the required water diffusion coefficient through membrane is insignificant.

The value of the diffusion coefficient for real materials is no function of current density. Therefore, the simulated values of diffusion coefficient give an information on the minimum diffusion coefficient a membrane needs in order to allow operation up to the given current. In the investigated range of current density, the required water diffusion coefficients for all conditions are for example far below those observed for the proton exchange membrane Nafion, $D_{H_2O}^{Naf}(323\text{ K}) = 4.6 \cdot 10^{-6} \text{ cm}^2 \text{ s}^{-1}$ [31]. The only research paper about water diffusion through an anion exchange membrane published so far [12] shows diffusion coefficients close to those of Nafion for 303 K and 313 K. Hence, it may be expected that the water diffusion coefficient through an anion exchange membrane is sufficient to supply sufficient water for cathode reaction.

Nevertheless, there will be a discrepancy between the required and the actual diffusion coefficient of water. If the actual diffusion coefficient is higher than the required one, water is accumulated at the cathode and the assumption $c_{H_2O}^C = 0$ is no longer valid. Consequently, the concentration gradient decreases and water diffusion is diminished. Nevertheless, it is possible that some pores of catalyst layer or gas diffusion layer at the cathode get blocked by liquid water which would lead to a decrease in cell performance.

If the actual diffusion coefficient is below the required one, water transport through membrane is not sufficient for cathodic water supply. Either the lacking water has to be taken from the gas

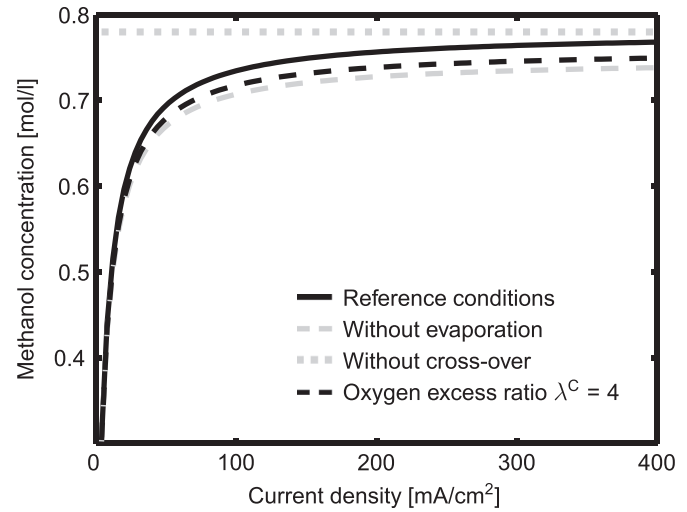


Fig. 7. Methanol concentration in liquid phase at anode in scenario 2 at reference conditions: Including electro-osmotic water drag, methanol cross-over and evaporation at cathode with an air excess ratio of $\lambda^C = 10$; and for three other cases that differ from reference conditions in one of the mentioned conditions.

or the current density has to be reduced until the water diffusion is sufficient.

The resulting methanol concentrations in the liquid phase at anode as a function of current density are displayed in Fig. 7. In the case without methanol cross-over, methanol concentration does not change with current density. This can be explained as follows: All inlet volume flow rates are proportional to current density due to their definition by constant excess ratios (see Eqs. (A.20) and (A.21)). Sources and sink terms consisting of reaction rates and the electro-osmotic drag of water (Eqs. (13)–(21)) are also proportional to current density. Since water diffusion is defined to be equal to water consumption at cathode, water diffusion is also proportional to current density. Hence, all terms needed to calculate outlet flow rates in Eqs. (11) and (12) are proportional to current density as well. Consequently, all terms of the molar balances (Eqs. (7) and (8)) in steady state with $\dot{n}_{\beta,\text{in}} = c_{\beta,\text{in}} F_{\text{in}}$ and $\dot{n}_{\beta,\text{out}} = c_{\beta,\text{out}} F_{\text{out}}$ are proportional to current density which can be

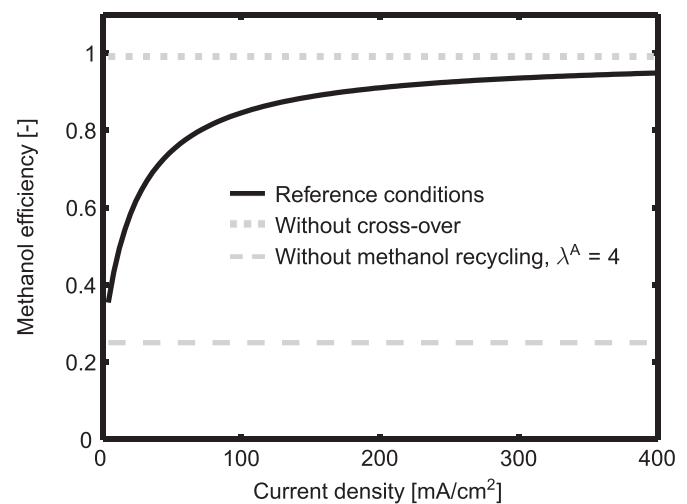


Fig. 8. Methanol efficiency in scenario 2 with a methanol excess ratio of $\lambda^A = 4$ at reference conditions with liquid recycling, without cross-over and without liquid recycling. Reference conditions: Including electro-osmotic water drag, methanol cross-over and evaporation at cathode with an air excess ratio of $\lambda^C = 10$.

cancelled. This results in a system of algebraic equations that is independent of current density and can be solved for steady state concentrations of components. Thus, all steady state concentrations are a function of excess ratios, inlet concentrations, concentrations of pure substances, water drag coefficient, pressure and temperature at anode and cathode but are independent of current density. However, the concentration of methanol in liquid phase at anode is below the inlet concentration, since methanol is consumed while water is produced by electrochemical reaction. Since methanol concentration is independent of current density, methanol efficiency is also independent of current density and is nearly 100% as shown in Fig. 8. The slight efficiency loss is caused by methanol evaporation at anode.

If methanol cross-over occurs, sources and sinks at cathode and, consequently, water diffusion and outlet volume flows contain terms that are not proportional to current density and concentrations are no longer independent of current density. The higher the current density, the smaller is the influence of the term independent of current density. As a consequence, the influence of methanol loss by cross-over is substantial at low current densities and causes small methanol concentrations and low efficiencies. At high current densities, methanol loss caused by cross-over is small compared to the other processes and methanol concentration converges to the value of the case without cross-over for high current densities.

In the three cases that include cross-over, methanol concentration differs slightly from that at reference conditions since the required water diffusion is smaller in case of lower air excess ratio $\lambda^C = 4$ or without evaporation and methanol dilution is more intense. However, the difference is small and the corresponding change in efficiency is insignificant. Hence, the methanol efficiency in Fig. 8 is only analysed for three different cases. The first two cases show methanol efficiency in reference conditions and without methanol cross-over assuming that all methanol at anodic exit can be recycled. The third case shows methanol efficiency without methanol recycling. Methanol cross-over causes high efficiency losses, especially for low current densities. Furthermore, high fuel efficiencies can only be achieved by recycling the methanol at anodic outlet. Since the methanol concentration for all cases shown in Fig. 7 is below the inlet concentration, recycling

of the methanol solution requires treatment to keep the methanol concentration constant and to avoid dilution.

The amount of water in the recycled liquid also needs to be considered. Fig. 9 shows the water accumulation at the anode which is calculated by Eq. (30). Both, negative and positive water accumulation are possible. In the case without evaporation, the required water diffusion is quite small and, therefore, more water is produced at anode than removed by diffusion. As a result, the water accumulation is positive because the amount of water leaving the anode is bigger than the amount of water fed to the anode. All other cases lead to a negative water accumulation which means that the molar flow of water at the anodic inlet is bigger than at the outlet. In these cases, the fuel cell runs out of water. This indicates that recycling the liquid phase at the anode will lead to another important challenge regarding water management in ADMFCs: the water level stabilisation.

5. Conclusions

As in most kinds of fuel cells, water management is a challenging topic in alkaline direct methanol fuel cells. Water is consumed at the gas-flushed cathode and produced at the anode where water is already in excess. In this paper, two scenarios of an ADMFC with different operation conditions are modelled and analysed in order to study conditions for sufficient water supply to cathode. Water management demands as well as the influence of processes like water drag and methanol cross-over on water management in ADMFCs are identified.

Scenario 1 reveals that humidifying cathodic inlet gas is not sufficient for water supply to cathode and it is important to consider water management at anode and water transport through membrane for any alkaline anion exchange membrane fuel cell. If water is only supplied by cathodic inlet, the air fed to cathode needs to be saturated with water and either high inlet temperatures or high volume flow rates are required to supply sufficient water. This is manageable for small systems operated in the lab for analysis, but it is unrealisable for real fuel cell systems that are supposed to work with high efficiency. Hence, the simulations reveal that water transport through membrane is essential and desired to supply sufficient water to the cathode for all alkaline anion exchange membrane fuel cells.

Scenario 2 shows that the required diffusion coefficient of water for sufficient water supply to the cathode of an ADMFC depends on operation conditions and rises with increasing current density. For membranes with a diffusion coefficient of water close to that of Nafion, water diffusion is sufficient to achieve current densities of $i \leq 400 \text{ mA cm}^{-2}$. Thus, additional humidification of cathodic inlet gas is necessary at high current densities, but for low current densities, humidification might cause flooding of cathode. Therefore, lack of water is not the reason for the low performance of present ADMFCs but flooding might be. The results also show the necessity to consider the diffusion coefficient of water when designing new membranes for alkaline fuel cells since water diffusivity is fixed by membrane material. The influence of methanol cross-over on the requirements placed on the membrane are negligible but electro-osmotic water drag and water evaporation at cathode have a significant effect. The latter depends on relative humidity of cathodic inlet gas, air excess ratio and the equilibrium of humidity of gas phase with the moistness of the membrane.

Stable water management at cathode of an ADMFC can be achieved by adjusting evaporation and current density. Furthermore, the operation range can be influenced by air excess ratio, water content of inlet air and also by membrane material.

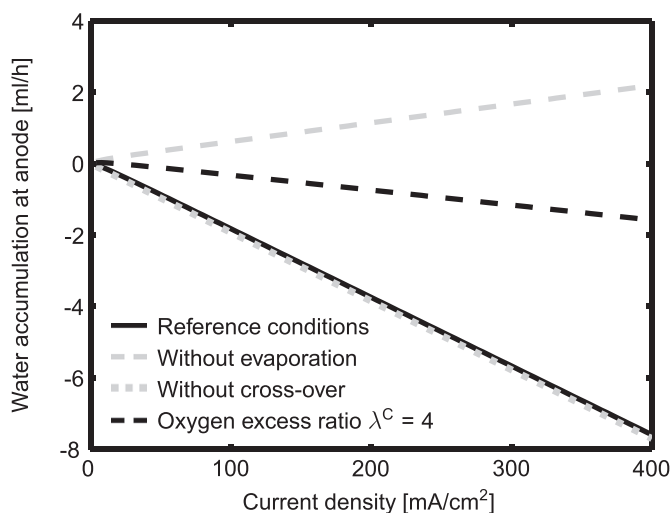


Fig. 9. Accumulation of liquid water at anode in scenario 2 at reference conditions: Including electro-osmotic water drag, methanol cross-over and evaporation at cathode with an air excess ratio of $\lambda^C = 10$; and for three other cases that differ from reference conditions in one of the mentioned conditions.

In order to achieve high methanol efficiencies, it is necessary to recycle methanol solution at the anodic outlet. However, it is not sufficient to consider methanol content in the recycled liquid but also water content is important since the fuel cell can run out of water or accumulate water depending on the operation conditions. Thus, water level stabilisation at the anode is another challenging topic for further studies.

Appendix A. Additional model equations

The following additional equations are used for the modelling of all scenarios described in this paper:

$$\dot{n}_{\text{Me}}^{\text{co}} = D_{\text{Me}}^{\text{M}} \frac{A^{\text{M}}}{d^{\text{M}}} c_{\text{Me,liq}}^{\text{A}} \quad (\text{A.1})$$

$$V_{\text{gas}}^{\text{A}} = \frac{\left(c_{\text{CO}_2}^{\text{A}} + c_{\text{Me}^{\text{g}}}^{\text{A}} + c_{\text{H}_2\text{O}^{\text{g}}}^{\text{A}} \right)}{c_{\text{gas}}^{\text{A}}} V^{\text{A}} \quad (\text{A.2})$$

$$V_{\text{liq}}^{\text{A}} = V^{\text{A}} - V_{\text{gas}}^{\text{A}} \quad (\text{A.3})$$

$$c_{\text{gas}}^{*\text{A/C}} = \frac{p^{\text{A/C}}}{R T^{\text{A/C}}} \quad (\text{A.4})$$

$$y_{\alpha}^{\text{A}} = X_{\alpha} \frac{p_{\alpha}^{\text{o}}(T^{\text{A}})}{p^{\text{A}}} \quad (\text{A.5})$$

$$y_{\alpha(\text{in})}^{\text{C}} = R H_{(\text{in})}^{\text{C}} \frac{p_{\alpha}^{\text{o}}(T_{(\text{in})}^{\text{C}})}{p_{(\text{in})}^{\text{C}}} \quad (\text{A.6})$$

$$X_{\text{H}_2\text{O}} = \frac{c_{\text{H}_2\text{O}}^{\text{A}}}{c_{\text{Me}}^{\text{A}} + c_{\text{H}_2\text{O}}^{\text{A}}} \quad (\text{A.7})$$

$$X_{\text{Me}} = 1 - X_{\text{H}_2\text{O}} \quad (\text{A.8})$$

$$p_{\alpha}^{\text{o}}(T) = p^{\text{crit}} \exp \left[\frac{1}{T_{\text{r}}} \left(A(1 - T_{\text{r}}) + B(1 - T_{\text{r}})^{1.5} + C(1 - T_{\text{r}})^3 + D(1 - T_{\text{r}})^6 \right) \right] \quad (\text{A.9})$$

$$T_{\text{r}} = \frac{T}{T^{\text{crit}}} \quad (\text{A.10})$$

$$c_{\text{H}_2\text{O}^{\text{g,in}}}^{\text{C}} = y_{\text{H}_2\text{O}^{\text{g,in}}}^{\text{C}} c_{\text{gas,in}}^{\text{C}} \quad (\text{A.11})$$

$$c_{\text{O}_2,\text{in}}^{\text{C}} = 0.21 \left(1 - y_{\text{H}_2\text{O}^{\text{g,in}}}^{\text{C}} \right) c_{\text{gas,in}}^{\text{C}} \quad (\text{A.12})$$

$$c_{\text{N}_2,\text{in}}^{\text{C}} = 0.79 \left(1 - y_{\text{H}_2\text{O}^{\text{g,in}}}^{\text{C}} \right) c_{\text{gas,in}}^{\text{C}} \quad (\text{A.13})$$

Thereby, the vapour pressure in Eq. (A.9) is described by the Wagner equation [30].

The concentrations of liquid methanol c_{Me}^{A} and water $c_{\text{H}_2\text{O}}^{\text{A}}$ at anode are based on the volume of the whole anode chamber which includes gas and liquid phase. For calculating diffusion of methanol and water the concentrations based on liquid volume only are needed. These can be calculated as follows:

$$c_{\text{Me,liq}}^{\text{A}} = \frac{n_{\text{Me}}^{\text{A}}}{V_{\text{liq}}^{\text{A}}} = \frac{c_{\text{Me}}^{\text{A}} V^{\text{A}}}{V_{\text{liq}}^{\text{A}}} \quad (\text{A.14})$$

$$c_{\text{H}_2\text{O,liq}}^{\text{A}} = \frac{n_{\text{H}_2\text{O}}^{\text{A}}}{V_{\text{liq}}^{\text{A}}} = \frac{c_{\text{H}_2\text{O}}^{\text{A}} V^{\text{A}}}{V_{\text{liq}}^{\text{A}}} \quad (\text{A.15})$$

The flow rates entering or leaving anode or cathode are described by:

$$\dot{n}_{\alpha,\text{in}}^{\text{A}} = c_{\alpha,\text{in}}^{\text{A}} F_{\text{in}}^{\text{A}} \quad (\text{A.16})$$

$$\dot{n}_{\text{dry,in}}^{\text{C}} = \frac{\lambda^{\text{C}}}{0.21} \frac{A^{\text{M}} i}{4F} \quad (\text{A.17})$$

$$\dot{n}_{\text{dry,out}}^{\text{C}} = \dot{n}_{\text{dry,in}}^{\text{C}} + \sigma_{\text{O}_2}^{\text{C}} + \sigma_{\text{CO}_2}^{\text{C}} + \sigma_{\text{N}_2}^{\text{C}} \quad (\text{A.18})$$

$$\dot{n}_{\text{H}_2\text{O}^{\text{g,in/out}}}^{\text{C}} = \frac{y_{\text{H}_2\text{O}^{\text{g,in/out}}}^{\text{C}}}{1 - y_{\text{H}_2\text{O}^{\text{g,in/out}}}^{\text{C}}} \dot{n}_{\text{dry,in/out}}^{\text{C}} \quad (\text{A.19})$$

$$F_{\text{in}}^{\text{A}} = \frac{\lambda^{\text{A}}}{c_{\text{Me,in}}^{\text{A}}} \frac{A^{\text{M}} i}{6F} \quad (\text{A.20})$$

$$F_{\text{in}}^{\text{C}} = \frac{\lambda^{\text{C}}}{c_{\text{O}_2,\text{in}}^{\text{C}}} \frac{A^{\text{M}} i}{4F} \quad (\text{A.21})$$

In Scenario 1 (Section 4.1) the remaining concentration of water in the cathode chamber is calculated by including a diffusion layer. The diffusive molar flow of water is equal to the water consumption by reaction. Therefore, the minimal required water concentration can be calculated by:

$$c_{\text{H}_2\text{O}^{\text{g}}}^{\text{C}} = \frac{i}{2F} \frac{d^{\text{GDL}}}{D_{\text{H}_2\text{O}^{\text{g}}}^{\text{GDL}}} \quad (\text{A.22})$$

This concentration is also needed for the calculation of the required air excess ratio λ^{C} in Eq. (26) that is derived in the following:

Including Eqs. (23)–(25) in Eq. (12) for $\dot{n}_{\text{H}_2\text{O}^{\text{g}}}^{\text{diff}} = 0$ results in:

$$F_{\text{out}}^{\text{C}} = \frac{p_{\text{in}}^{\text{C}} T_{\text{in}}^{\text{C}}}{p^{\text{C}} T_{\text{in}}^{\text{C}}} F_{\text{in}}^{\text{C}} + \left(-\frac{1}{c_{\text{O}_2}^{\text{C}}} - \frac{2}{c_{\text{H}_2\text{O}^{\text{g}}}^{\text{C}}} \right) \frac{A^{\text{M}} i}{4F} \quad (\text{A.23})$$

Combining Eqs. (A.21), (A.11) and (A.12), the molar flux of water entering the cathode chamber is calculated by:

$$\begin{aligned} \dot{n}_{\text{H}_2\text{O}^{\text{g,in}}}^{\text{C}} &= F_{\text{in}}^{\text{C}} c_{\text{H}_2\text{O}^{\text{g,in}}}^{\text{C}} \\ &= \frac{\lambda^{\text{C}}}{0.21 \left(1 - y_{\text{H}_2\text{O}^{\text{g,in}}}^{\text{C}} \right) c_{\text{gas,in}}^{\text{C}}} \frac{A^{\text{M}} i}{4F} y_{\text{H}_2\text{O}^{\text{g,in}}}^{\text{C}} c_{\text{gas,in}}^{\text{C}} \\ &= \frac{\lambda^{\text{C}}}{0.21} \frac{y_{\text{H}_2\text{O}^{\text{g,in}}}^{\text{C}}}{1 - y_{\text{H}_2\text{O}^{\text{g,in}}}^{\text{C}}} \frac{A^{\text{M}} i}{4F} \end{aligned} \quad (\text{A.24})$$

$$\begin{aligned}
0 &= \frac{\lambda^C}{0.21} \frac{y_{H_2Og, in}^C}{1 - y_{H_2Og, in}^C} \frac{A_M i}{4F} - c_{H_2Og}^C \left(\frac{p_{in}^C T_{in}^C R}{p_{in}^C T_{in}^C R} \frac{\lambda^C}{0.21(1 - y_{H_2Og, in}^C) c_{gas, in}^C} - \frac{3}{c_{gas}^C} \right) \frac{A_M i}{4F} - \frac{A_M i}{2F} \\
0 &= \frac{A_M i}{4F} \left(\frac{\lambda^C}{0.21} \frac{y_{H_2Og, in}^C}{1 - y_{H_2Og, in}^C} - \frac{c_{H_2Og}^C}{c_{gas}^C} \frac{\lambda^C}{0.21(1 - y_{H_2Og, in}^C)} + \frac{3c_{H_2Og}^C}{c_{gas}^C} - 2 \right) \\
0 &= \frac{\lambda^C}{0.21} \frac{1}{1 - y_{H_2Og, in}^C} \left(y_{H_2Og, in}^C - \frac{c_{H_2Og}^C}{c_{gas}^C} \right) + 3 \frac{c_{H_2Og}^C}{c_{gas}^C} - 2 \\
\Rightarrow 2 - 3 \frac{c_{H_2Og}^C}{c_{gas}^C} &= \frac{\lambda^C}{0.21} \frac{1}{1 - y_{H_2Og, in}^C} \left(y_{H_2Og, in}^C - \frac{c_{H_2Og}^C}{c_{gas}^C} \right) \\
\Rightarrow \lambda^C &= 0.21 \left(1 - y_{H_2Og, in}^C \right) \frac{2 - 3 \frac{c_{H_2Og}^C}{c_{gas}^C}}{y_{H_2Og, in}^C - \frac{c_{H_2Og}^C}{c_{gas}^C}}
\end{aligned} \tag{A.25}$$

For ideal gases, concentrations of pure gases are equal at the same conditions $c_{O_2}^{*C} = c_{H_2Og}^{*C} = c_{gas}^C$ and Eq. (26) can be derived by combining Eqs. (A.23), (A.24) and (22):

Nomenclature

Latin symbols

A^M	area of membrane [m^2]
A	Wagner coefficient for vapour pressure [-]
B	Wagner coefficient for vapour pressure [-]
C	Wagner coefficient for vapour pressure [-]
c_β	concentration of component β [$mol l^{-1}$]
c_β^*	concentration of pure substance β [$mol l^{-1}$]
D	Wagner coefficient for vapour pressure [-]
D_β^M	diffusion coefficient of component β through membrane [$m^2 s^{-1}$]
d^M	thickness of membrane [m]
F	Faraday constant [$A s mol^{-1}$]
$F_{in/out}$	volume flow rate at inlet/outlet [$m^3 s^{-1}$]
i	current density [$A m^{-2}$]
$j_{k,\beta}$	diffusion flux of β in direction k [$kg m^{-2} s$]
n_β	molar flow of component β [$mol s^{-1}$]
p	pressure [Pa]
p^{crit}	critical pressure [Pa]
$p_\beta^0(T)$	vapour pressure of β at temperature T [Pa]
RH	relative humidity [%]
T	temperature [K]
T^{crit}	critical temperature [K]
T_r	temperature referred to critical temperature [-]
t	time [s]
t_{max}	maximal simulated operation time [s]
V	volume [m^3]
v_k	velocity in direction k [$m s^{-1}$]
y	mole fraction in gas phase [-]

X	mole fraction in liquid phase [-]
z_k	space coordinate in direction k [m]

Greek symbols

κ	water drag coefficient [-]
λ	excess ratio of reactant [-]
ρ_β	density of component β [$mol l^{-1}$]
σ_β^*	mass sources and sinks of component β [$kg s^{-1}$]
σ_β	molar sources and sinks of component β [$mol s^{-1}$]

Superscripts

A	at anode
C	at cathode
co	cross-over
$crit$	critical value
$diff$	diffusion
$drag$	electro-osmotic water drag
exc	excess
M	of membrane
Sys	system

Subscripts

α	component in anode chamber
β	component general
γ	component in cathode chamber
dry	dry gas
k	spatial direction
N	at norm conditions
in	at inlet
liq	of liquid phase
out	at outlet
Me	liquid methanol
Me^g	methanol vapour
CO_2	carbon dioxide
H_2O	liquid water
H_2Og	water vapour
N_2	nitrogen

O₂ oxygen

Abbreviations

AAEM	alkaline anion exchange membrane
ADMFC	alkaline direct methanol fuel cell
AFC	alkaline fuel cell
CSTR	continuous stirred tank reactor
FC	fuel cell

References

- [1] E.H. Yu, U. Krewer, K. Scott, *Energies* 3 (2010) 1499–1528.
- [2] E.H. Yu, X. Wang, U. Krewer, L. Li, K. Scott, *Energy Environ. Sci.* 5 (2012) 5668–5680.
- [3] A. Tewari, V. Sambhy, M. Macdonald, A. Sen, *J. Power Sources* 153 (2006) 1–10.
- [4] H. Ko, H. Juang, *J. Appl. Electrochem.* 13 (1983) 725–730.
- [5] J. Varcoe, R. Slade, E. Lam How Yee, *Chem. Commun.* (2006) 1428–1429.
- [6] L.A. Adams, S.D. Poynton, C. Tamain, R.C.T. Slade, J.R. Varcoe, *ChemSusChem* 1 (2008) 79–81.
- [7] E. Yu, K. Scott, *J. Power Sources* 137 (2004) 248–256.
- [8] L. Sun, J. Guo, J. Zhou, Q. Xu, D. Chu, R. Chen, *J. Power Sources* 202 (2012) 70–77.
- [9] N. Fujiwara, Z. Siroma, S.-i. Yamazaki, T. Ioroi, H. Senoh, K. Yasuda, *J. Power Sources* 185 (2008) 621–626.
- [10] J.R. Varcoe, M. Beillard, D.M. Halepoto, J.P. Kizewski, S.D. Poynton, R.C.T. Slade, *ECS Trans.* 16 (2008) 1819–1834.
- [11] S.D. Poynton, J.P. Kizewski, R.C.T. Slade, J.R. Varcoe, *Solid State Ionics* 181 (2010) 219–222, 14th International Conference on Solid State Protonic Conductors (SSPC-14), Kyoto, Japan, Sep 07–11, 2008.
- [12] Y.S. Li, T.S. Zhao, W.W. Yang, *Int. J. Hydrogen Energy* 35 (2010) 5656–5665.
- [13] N. Follain, S. Roualde, S. Marais, J. Frugier, M. Reinholdt, J. Durand, *J. Phys. Chem. C* 116 (2012) 8510–8522.
- [14] T.D. Myles, A.M. Kiss, K.N. Grew, A.A. Peracchio, G.J. Nelson, W.K.S. Chiu, *J. Electrochem. Soc.* 158 (2011) B790–B796.
- [15] T. Yamanaka, T. Takeguchi, H. Takahashi, W. Ueda, *J. Electrochem. Soc.* 156 (2009) B831–B835.
- [16] I. Verhaert, S. Verhelst, G. Janssen, G. Mulder, M. De Paepe, *Int. J. Hydrogen Energy* 36 (2011) 11011–11024.
- [17] S. Rowshan Zamir, M. Kazemeini, M. Isfahani, *Int. J. Hydrogen Energy* 23 (1998) 499–506.
- [18] P. Björnbom, S. Yang, *Electrochim. Acta* 38 (1993) 2599–2609.
- [19] S. Yang, P. Björnbom, *Electrochim. Acta* 37 (1992) 1831–1843.
- [20] S. Huo, H. Deng, Y. Chang, K. Jiao, *Int. J. Hydrogen Energy* 37 (2012) 18389–18402.
- [21] H. Deng, S. Huo, Y. Chang, Y. Zhou, K. Jiao, *Int. J. Hydrogen Energy* 38 (2013) 6509–6525.
- [22] M. Kimble, R. White, *J. Electrochim. Soc.* 138 (1991) 3370–3382.
- [23] J. Jo, S. Moon, S. Yi, *J. Appl. Electrochem.* 30 (2000) 1023–1031.
- [24] S. Mohan, S.O.B. Shrestha, *J. Fuel Cell Sci. Technol.* 7 (2010).
- [25] I. Verhaert, M. De Paepe, G. Mulder, *J. Power Sources* 193 (2009) 233–240.
- [26] A. Verma, S. Basu, *J. Power Sources* 168 (2007) 200–210.
- [27] K.N. Grew, W.K.S. Chiu, *J. Electrochim. Soc.* 157 (2010) B327–B337.
- [28] K.N. Grew, D. Chu, W.K.S. Chiu, *J. Electrochim. Soc.* 157 (2010) B1024–B1032.
- [29] C.Y. Du, T.S. Zhao, W.W. Yang, *Electrochim. Acta* 52 (2007) 5266–5271.
- [30] Verein Deutscher Ingenieure, VDI-Gesellschaft Verfahrenstechnik und Chemie-Ingenieurwesen GVC (Ed.), *VDI-Wärmeatlas*, Springer-Verlag, Berlin, Heidelberg, New York, 2006.
- [31] S. Yeo, A. Eisenberg, *J. Appl. Polym. Sci.* 21 (1977) 875–898.